



# Electron backscatter diffraction characterization of laser-induced periodic surface structures on nickel surface

Xxx Sedao<sup>a,\*</sup>, Claire Maurice<sup>b</sup>, Florence Garrelie<sup>a</sup>, Jean-Philippe Colombier<sup>a</sup>,  
Stéphanie Reynaud<sup>a</sup>, Romain Quey<sup>b</sup>, Gilles Blanc<sup>b</sup>, Florent Pigeon<sup>a</sup>

<sup>a</sup> Laboratoire Hubert Curien, Université Jean Monnet, 42000 St-Etienne, France

<sup>b</sup> Laboratoire Georges Friedel, Ecole Nationale Supérieure des Mines, 42023 St-Etienne, France

## ARTICLE INFO

### Article history:

Received 28 June 2013

Received in revised form 24 October 2013

Accepted 25 October 2013

Available online 1 November 2013

### Keywords:

LIPSS

Ripples

Ultrafast laser

Femtosecond pulse

EBS

## ABSTRACT

We report on the structural investigation of laser-induced periodic surface structures (LIPSS) generated in polycrystalline nickel target after multi-shot irradiation by femtosecond laser pulses. Electron backscatter diffraction (EBSD) is used to reveal lattice rotation caused by dislocation storage during LIPSS formation. Localized crystallographic damages in the LIPSS are detected from both surface and cross-sectional EBSD studies. A surface region (up to 200 nm) with 1–3° grain disorientation is observed in localized areas from the cross-section of the LIPSS. The distribution of the local disorientation is inhomogeneous across the LIPSS and the subsurface region.

© 2013 Elsevier B.V. All rights reserved.

## 1. Introduction

The formation of laser-induced periodic surface structures (LIPSS), often referred to as ripples, has been observed on the surface of semiconductors, metals, and dielectrics for a broad range of laser parameters [1–4]. On metals, the LIPSS formation may be attributed to an initial optical modulation effect at the surface [1]. A material instability effect upon ultrafast laser irradiation may also contribute to LIPSS formation at the surface [5]. The optic effect of initial modulation gives rise to inhomogeneous energy absorption at the illuminated surface [1,6]. Following localized photo-excitation, a rapid change in the lattice temperature can result in the development of thermal stresses and/or fast phase transition [7]. Evidence of stress loading and fast phase transition, such as formation of lattice defects and amorphization, has been observed in various material systems using transmission electron microscopy (TEM) based techniques [8–11]. However, quantification and spatial distribution of aforementioned microstructural modifications, which are of great importance for understanding LIPSS formation, are still elusive. The purpose of this paper is to analyze, for the first time, lattice deformation and its distribution in the vicinity of LIPSS and its subsurface region. Similar to TEM, high resolution EBSD is one of the few techniques with sufficient

sensitivity for lattice defect detection and phase discrimination at nanometer scale [12]. The present study benefits from the special strength of EBSD in analyzing the extent of lattice defect, such as plane defects and crystal disorientation, and mapping the locations of orientation gradients [13].

## 2. Experimental

The material used in this study is a polycrystalline nickel disk Ø 50 mm and 3 mm thick. The sample was prepared by conventional metallographic procedures with a final polish of 0.25 µm diamond suspension followed by vibratory polishing in 0.25 µm colloidal silica solution for about 45 min. The LIPSS on the nickel substrate were produced using a Ti: Sapphire femtosecond laser system (Legend Coherent Inc.). The laser has a central wavelength of 800 nm with a pulse duration of 50 fs and a repetition rate of 1 kHz. Before delivery onto the surface of the nickel sample, the laser pulses were linearly polarized attenuated through a pair of neutral density filters. A Pockels unit cell is used to control the total number of laser pulses. The laser beam is focused normally, through an achromatic lens onto the sample that is vertically mounted on an X–Y motorized translation stage. The dimension of the beam spot on sample surface,  $2w_0 = 90 \mu\text{m}$  ( $1/e^2$  intensity), is determined by single shot D-square method [14]. In cross-sectional EBSD study, the cross-section sample of the LIPSS was prepared by the site-specific focused ion beam (FIB) technique [15]. A layer of a few 100 nm thick tungsten was deposited to protect the surface of the laser impact

\* Corresponding author. Tel.: +33650434065.

E-mail address: [sedao.xxx@gmail.com](mailto:sedao.xxx@gmail.com) (X. Sedao).

during FIB process. The sample was then milled with a focused ion beam of 30 keV gallium atoms and lift-out technique was employed to extract the thin lamella from the surrounding milled area. After the extraction, the lamella was welded onto a TEM copper grid, which was later mounted on a SEM sample stub. This allowed morphology observation using SEM and the investigation of the final crystalline state of the material using EBSD.

The analysis of surface modification in laser impact area was performed using a scanning electron microscope (SEM, Zeiss Supra55 FEG-SEM), equipped with an HKL-Oxford Instruments EBSD system composed of a Nordlys II camera and Channel 5 software suit. EBSD acquisitions were performed with the accelerating voltage varying from 7 to 20 kV, with a working distance of 15 mm and sample tilt of  $70^\circ$  with respect to horizontal. The spatial resolution of the EBSD is typically about  $20 \times 60 \times 10$  (horizontal axis  $\times$  tilted axis  $\times$  depth, all units in nm) [16]. Direct interrogation of EBSD pattern (EBSP) and local crystal disorientation (LCD) derived from the EBSD analysis are used to analyze the lattice distortions induced by ultrafast irradiation. For cross-sectional study, which will be explained further below, the EBSD data was acquired at 10 nm step size. The local crystal disorientation through texture component function available in the EBSD data analysis software was employed to analyze the crystallographic change after LIPSS formation. The LCD maps illustrate the crystal rotation at each point with respect to a reference site deep into the substrate, providing a good representation of the overall distribution of disorientation induced by lattice distortion [17,18].

### 3. Results and discussion

As discussed before, change in crystalline structure and dislocations at surfaces can be expected upon laser irradiation. These modifications can be revealed from EBSP (also known as Kikuchi diffraction pattern [19]) analysis. For instance, an EBSD study at a flat surface region in the vicinity of the LIPSS can readily reveal the impact of laser irradiation. Fig. 1a shows the SEM image of a nickel surface with its central part (indicated by white-colored circle) irradiated by 20,000 laser pulses at a peak fluence of  $10 \text{ mJ}/\text{cm}^2$ . The laser process condition employed here assures that the LIPSS appear only at the central part while the surrounding of the LIPSS within the laser illuminated area remains flat (therefore surface EBSD analysis can be applied). Due to the Gaussian profile of the laser spot, only at the central part of the irradiated area the local laser fluence was intense enough to cause surface morphology change. In order to visualize the micro-structural change induced by laser irradiation, EBSPs are acquired from two different locations on the surface, on a flat surface area close to the LIPSS and outside the central part of laser irradiated area. These locations are marked with rectangles, number 1- and 2-indexed in Fig. 1a, and their EBSPs are shown in Fig. 1b and c, respectively. The EBSP from the area outside the central part of laser irradiation zone, as shown in Fig. 1b, is the superimposed Kikuchi diffraction bands, generated from different lattice diffracting planes of nickel. It is hard to see any discernible features in the EBSP acquired from the vicinity of the LIPSS (Fig. 1c), indicating a compromise of the diffraction conditions (atomic arrangement of the lattice). The diffuseness of the EBSP could be explained by the accumulation of dislocations (either from plastic deformation or rapid solidification of a melted layer) or the presence of an amorphous phase. The EBSD data can be acquired from the entire sample surface, then indexed and used for generating surface maps for more comprehensive and diverse studies. Analysis through EBSD mapping is applied in the cross-section study, as described in the following.

As the backscatter electrons come from a skin layer of  $\sim 10 \text{ nm}$  from the surface, EBSD analysis provides information only from

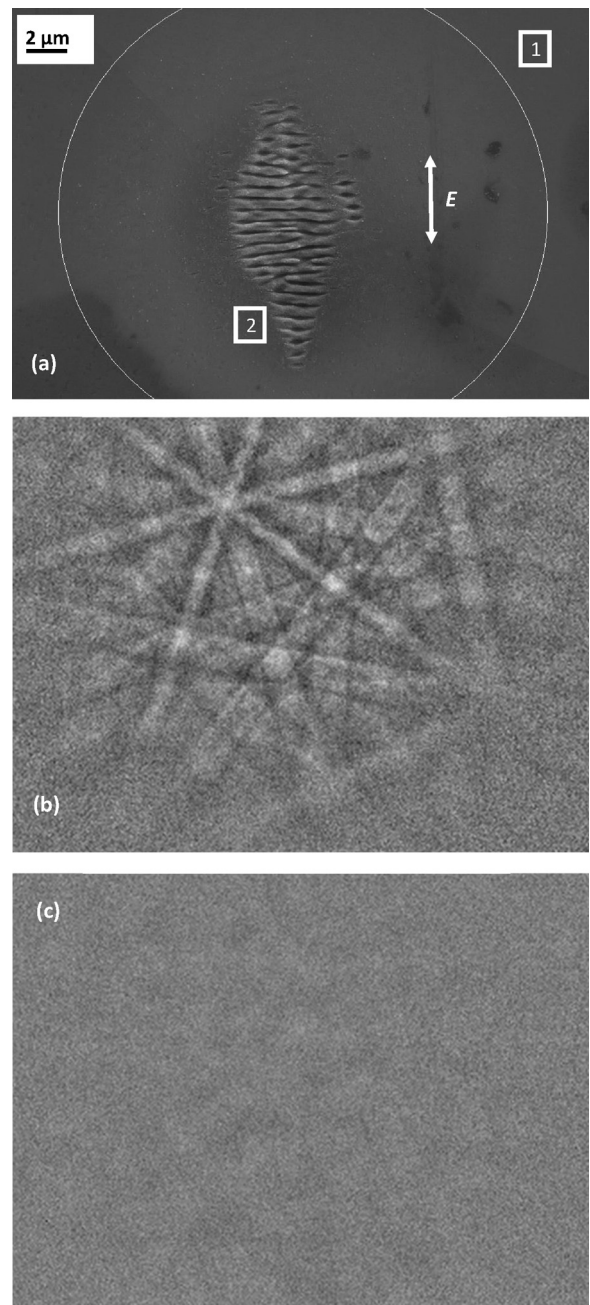


**Fig. 1.** (a) SEM image of the nickel surface. The circular area marked in the image received laser pulses. The laser polarization is indicated in the figure by the white arrow and letter *E*. The EBSD diffraction patterns from the number-indexed areas (1) and (2) are shown in (b) and (c).

the very surface. This means EBSD study merely from the surface of LIPSS is not sufficient, as the peak-to-valley amplitude of LIPSS is often in the range of a few tens to 100 nm and crystalline damage could expand a few tens of nm into the subsurface region of LIPSS [11]. In order to obtain micro-structural information from entire LIPSS and their subsurface region, cross-section samples perpendicular to the LIPSS are analyzed. The SEM surface image shown in Fig. 2a is the laser impact prepared for the cross-sectional study. The impact was produced with a peak fluence of  $0.47 \text{ J}/\text{cm}^2$  and 50 laser pulses. Fig. 2b shows a reconstructed EBSD surface map representing surface normal-projected, color-coded inverse pole figure (IPF), of the same area as observed in Fig. 2a, c is the color-coding of the IPF in Fig. 2b, indicating stereographic projection of

Download English Version:

<https://daneshyari.com/en/article/5351610>

Download Persian Version:

<https://daneshyari.com/article/5351610>

[Daneshyari.com](https://daneshyari.com)